Quaternary Science Reviews 203 (2019) 141–150

Contents lists available at ScienceDirect

Quaternary Science Reviews

journal homepage: www.elsevier.com/locate/quascirev

Reconciling the onset of deglaciation in the upper Rangitata valley, Southern Alps, New Zealand

David J.A. Barrell [a, *], Aaron E. Putnam [b], George H. Denton [b]

[a] GNS Science, Private Bag 1930, Dunedin, 9054, New Zealand
[b] School of Earth and Climate Sciences and Climate Change Institute, University of Maine, Orono, ME, 04469, USA

ARTICLE INFO

Article history:
Received 29 July 2018
Received in revised form
2 November 2018
Accepted 2 November 2018

Keywords:
Beryllium-10
Moraine chronology
New Zealand
Last glacial termination
Paleoclimate

ABSTRACT

Enquiry into the detailed timing of paleoclimate events depends on well-resolved and reliable chronologies. A recently published set of ^{10}Be surface-exposure ages for moraine boulders in the upper Rangitata valley was interpreted to indicate a gradual reduction in glacier surface height between c. 21 and c. 17 ka, without rapid glacier recession beginning c. 18 ka as reported from other valleys. The dating results were suggested to be consistent with moraine geomorphology and an interpreted lack of post-glacial lake formation in the valley. In contrast, we argue that the geomorphology is consistent with sustained glacier recession and we highlight evidence for a post-glacial lake. Furthermore, the upper Rangitata moraine chronology was encumbered by inaccurate altitude values assigned to many of the sample sites. Recalculation of the ^{10}Be ages using accurate elevations produces values that are as much as 3000 years younger than originally reported. The recalculated values indicate no significant age difference across the c. 300-m relative altitudinal spread of sample locations, with mean age of all samples c. 17.7 ± 0.3 ka. The previous inference of slow late-glacial ice retreat is not supported by the recalculated chronology. Rather, the revised glacial chronology implies that substantial ice-surface lowering of the Last Glacial Maximum Rangitata glacier was in progress shortly after c. 18 ka. The revised upper Rangitata chronology is compatible with dating from other eastern valleys of the Southern Alps, indicating moraine formation at c. 18 ka, followed by sustained glacier recession associated with regional climatic amelioration.

© 2018 Elsevier Ltd. All rights reserved.

1. Introduction

Improved understanding of past climate changes depends on high-quality chronological control. In-situ produced terrestrial cosmogenic nuclide surface-exposure dating (SED) of climate-related landforms has become an increasingly valuable tool for paleoclimate enquiry. Over the past decade, well resolved ^{10}Be SED chronologies have been published for several major formerly-glaciated valleys in the Southern Alps of New Zealand. The growing body of SED moraine chronologies provides an important paleoclimate record from the landforms of highly-responsive valley glaciers at this key Southern Hemisphere mid-latitude location (Barrell, 2011; Darvill et al., 2016 and references therein). The publication of ^{10}Be SED ages for Last Glacial Maximum (LGM) moraines in the upper Rangitata valley in the eastern (leeward) sector of the mountain range (Shulmeister et al., 2018) adds to an existing SED moraine chronology from the Clearwater distributary lobe of the LGM Rangitata glacier (Rother et al., 2014), whose dataset includes three ages from the downstream end of the upper Rangitata valley (Fig. 1). Both those studies concluded that there was slow retreat of the Rangitata glacier during the LGM (adopted here as c. 27–18 ka, modified from Clark et al., 2009), with sustained deglacial recession not commencing until sometime after c. 17 ka (Shulmeister et al., 2018). This contrasts with findings from nearby Southern Alps glacial valleys. Moraine dating in the Rakaia and Ohau valleys (Putnam et al., 2013a, 2013b) indicates that rapid and sustained glacier recession began at c. 18 ka and each glacier lost at least 40% of its length within no more than c. 1000 years. The Rakaia and Ohau results are similar to findings in southwestern South America. In the Chilean Lake District, after the last major ice advance culminated at c. 18 ka, the Licán ignimbrite was deposited across the lower to middle reaches of several glacial valleys at c. 16.8 ka, demonstrating that by then, ice had retreated well back into the mountains (Moreno et al., 2015). On Tierra Del Fuego, ice

* Corresponding author.
E-mail address: d.barrell@gns.cri.nz (D.J.A. Barrell).

https://doi.org/10.1016/j.quascirev.2018.11.003
0277-3791/© 2018 Elsevier Ltd. All rights reserved.

was back to near-modern glacier limits by c. 16.5 ka (Hall et al., 2013, 2017).

If the SED-based glacial chronology of the upper Rangitata valley is a reliable indicator of regional climate patterns, it implies that rapid ice recession in other Southern Alps valleys at ~18 ka was due to factors other than direct climate forcing (Shulmeister et al., 2018). The chronology of Southern Alps deglaciation bears directly on a very important question; what caused the last glacial termination in the Southern Alps and, more generally, in the middle latitudes of the Southern Hemisphere? Quite different causative mechanisms could emerge if there was an episode of rapid climatic warming beginning shortly after 18 ka, or if the overall warming was more gradual without such an episode. In this paper, we review information from the upper Rangitata valley pertaining to the onset of post-LGM deglaciation, with emphasis on assessing the accuracy of the recently published SED age determinations.

2. Review of dating results and interpretations

The upper Rangitata SED chronology was obtained from 23 erratic boulders on moraines on the true right side of the upper Rangitata valley (Shulmeister et al., 2018). A statistical evaluation of the ages relative to the geomorphologic positions of the boulders was not provided and the discussion of dating results and interpretations comprised a few brief statements, for example in the caption of their Fig. 2: "*Average ages decline down-hill and up-valley but there is considerable overlap in ages*." In evaluating the dating results, we noted that the Shulmeister et al. (2018) sample locations can be placed into two geographical/geomorphological groups (Table 1). Twelve sample sites are clustered within an area of about 300 m by 600 m extent at higher elevation and we refer to these as the outer group. A set of 10 samples comes from lower elevations close to the Rangitata River valley floor, and we identify these as the inner group. There is one sample from a position intermediate between these two groups (Figs. 1–3).

A simple arithmetical mean of the reported ages is c. 20 ka for the outer group and c. 18 ka for the inner group (Table 2). Although Shulmeister et al. (2018) stated that an erosion-rate correction was not applied in their age calculations, we found that their data input file, archived in an external data repository identified here as Shulmeister (2018), did include an erosion rate of 0.0001 cm/yr (i.e. 1 mm/kyr). We ran a check by recalculating their data input values with that erosion rate, and successfully replicated the ages presented in their paper.

Sample location coordinates and elevations were not tabulated in the Shulmeister et al. (2018) paper bur rather were documented only in the Shulmeister (2018) data repository. There, we found significant discrepancies between the elevations assigned to many of the sample sites, compared to independent evidence. All the sample elevations from the outer moraine group, and two from the inner group, differ by typically more than 100 m from elevation contours on published topographic maps and ground elevations at each sample location from the digital elevation model (DEM) delivered in Google Earth (Table 1). All but one of the notably discrepant elevations are too low. For example, in the Shulmeister (2018) data input file, the outer group samples are assigned elevations between 515 and 584 m asl, but independent evidence indicate elevations of between 660 and 700 m asl. Of note, Fig. 2 of Shulmeister et al. (2018) displays 100-m interval topographic map contours and illustrates a 700 m above sea level (asl) contour in proximity to the outer group sample area, and their text indicates that the higher samples are from ~700 m asl. This suggests that data entry errors occurred in the input file for age calculations.

Sample elevation relative to sea level is a key parameter for calculating accurate SED ages, because SED ages are derived from the measured concentration of the target nuclide and the

Table 1
Sample ID, latitude (lat) and longitude (long) in decimal degrees, and elevations (Elev) in metres, of SED samples for the upper Rangitata valley. Latitude and longitude are taken from the Shulmeister (2018) data file, except for the outer group where locations were surveyed in March 2018. Elev S is the elevation value from the Shulmeister (2018) data repository. The other elevations are from this study, comprising Elev TC estimated from topographic contours, Elev SRTM estimated from the Satellite Radar Tracking Mission digital elevation model, and Elev dGPS measured using differential GPS. Elev TC and Elev dGPS are referenced to sea level, Elev SRTM to the WGS84 Earth Gravitational Model (EGM 96), and the datum for Elev S was not reported. The final column shows the difference between the Shulmeister (2018) elevations, and the Elev TC values, or Elev dGPS where available. For Elev TC ranges, the median of the range was used. Elevations in bold were used in age recalculation. We used the Elev S value where it is within 20 m of the Elev TC and Elev SRTM, otherwise the TC or dGPS elevations were used.

Sample ID	Lat (dd)	Long (dd)	Elev S (m)	Elev TC (m)	Elev SRTM (m)	Elev dGPS (m)	dGPS error (m)	Elev S minus Elev TC or Elev dGPS (m)
Samples from inner group of moraines								
BD1	−43.60983	170.87189	552	540	539	n/a	n/a	13
BD3	−43.60841	170.87635	**527**	520	520	n/a	n/a	7
BD4	−43.63979	170.88037	**605**	600	604	n/a	n/a	1
BD5	−43.61587	170.87686	614	**540**	540	n/a	n/a	74
BD6	−43.63387	170.87372	**631**	620–640	629	n/a	n/a	1
BD7	−43.61766	170.87896	**547**	540	540	n/a	n/a	7
BD8	−43.64915	170.8896	534	**560–580**	574	n/a	n/a	−36
BD9	−43.64985	170.89854	**537**	520–540	524	n/a	n/a	7
BD10	−43.64938	170.89842	**536**	520–540	521	n/a	n/a	6
BD11	−43.6481	170.89738	**533**	520–540	531	n/a	n/a	3
Sample from intermediate moraine								
BD-16-01	−43.68157	170.92627	**602**	600	594	n/a	n/a	2
Samples from outer group of moraines								
BD-16-02	−43.68262	170.88974	515	680–700	681	**692.0**	0.1	−177
BD-16-03	−43.68258	170.88956	516	680–700	681	**692.2**	0.1	−176
BD-16-04	−43.68182	170.88958	573	680–700	681	**688.6**	0.1	−116
BD-16-05	−43.68102	170.88769	575	680–700	683	**692.7**	0.1	−118
BD-16-06	−43.68075	170.88786	575	680–700	682	**690.1**	0.1	−115
BD-16-07	−43.68140	170.88653	578	680–700	691	**694.1**	0.1	−116
BD-16-08	−43.68012	170.88673	575	680–700	682	**692.4**	0.1	−117
BD-16-09	−43.68015	170.88688	575	680–700	682	**691.6**	0.1	−117
BD-16-10	−43.68002	170.88379	584	680–700	694	**700.7**	0.1	−117
BD-16-11	−43.67991	170.88386	584	680–700	691	**699.8**	0.1	−116
BD-16-12	−43.68011	170.88409	584	680–700	693	**699.4**	0.1	−115
BD-16-14	−43.68044	170.89203	560	660–680	668	**675.3**	0.8	−115

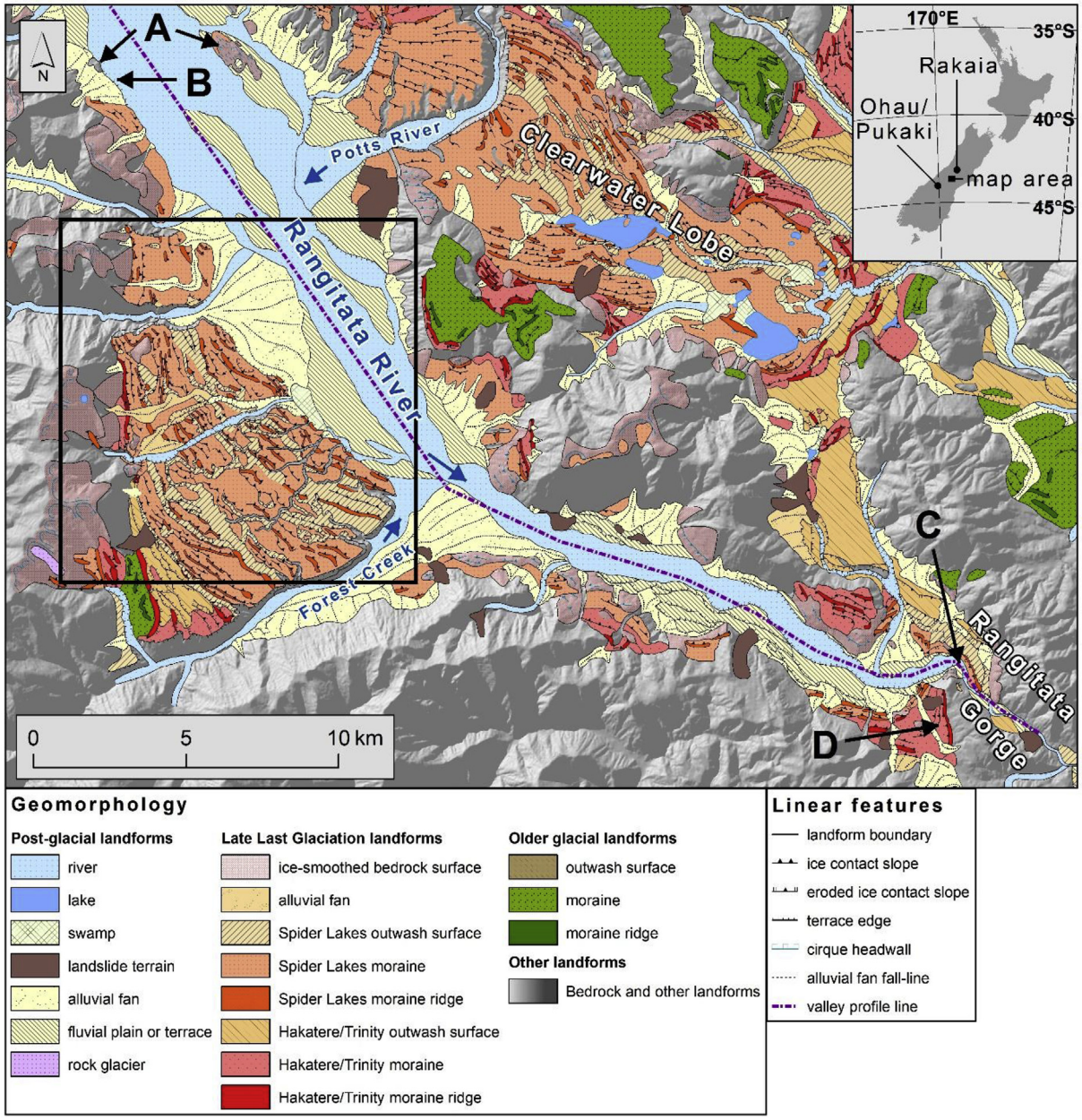

Fig. 1. Glacial geomorphological map of part of the upper Rangitata valley and adjacent areas, from the Barrell et al. (2011, 2013a) dataset, with location map inset. The black box shows the extent of Fig. 2. For the most part, the upper Rangitata valley floor is occupied by Holocene fluvial landforms, and A denotes the only two bedrock outcrops in this sector of the valley floor. B marks the position of a buried soil within alluvial fan deposits (Forsyth et al., 2003). Location C is the lake sediment dating site described by Mabin (1987) and illustrated in Fig. 6, while D is the location of three SED moraine boulder ages reported by Rother et al. (2014).

production rate of that nuclide, which depends on the cosmic radiation flux (Dunai and Stuart, 2009; Lifton et al., 2014). The flux reduces with decreasing elevation due to attenuation as a function of atmospheric density, hence the importance of accurate elevations. SED calculations using underestimated elevation values will overestimate the resulting ages. We have therefore taken the step of attempting to rectify the elevation errors and recalculate the ages for the upper Rangitata ^{10}Be dataset.

3. Methods

In this paper, we rely upon published literature, publicly-accessible information and personal field observations. We recalculated the ages of the Rangitata SED samples (Table 2) using the published ^{10}Be concentrations, shielding and sample thickness data of Shulmeister et al. (2018) and elevation values as explained below, in conjunction with the Balco et al. (2008) online calculator (UW online calculator version 2.3) and the Putnam et al. (2010) production rate calibration with 'Lm' scaling (e.g. Putnam et al., 2013a).

For elevation estimates, we examined sample locations in relation to 20-m interval topographic contours on the 1:50 000-scale Topo 50 map published by Land Information New Zealand, and the Satellite Radar Tracking Mission (SRTM) DEM accessible via Google Earth. The published topographic contours have been determined photogrammetrically relative to geodetic ground survey control. At the time of writing, the New Zealand Topo Map series is freely accessible for examination at www.topomap.co.nz.

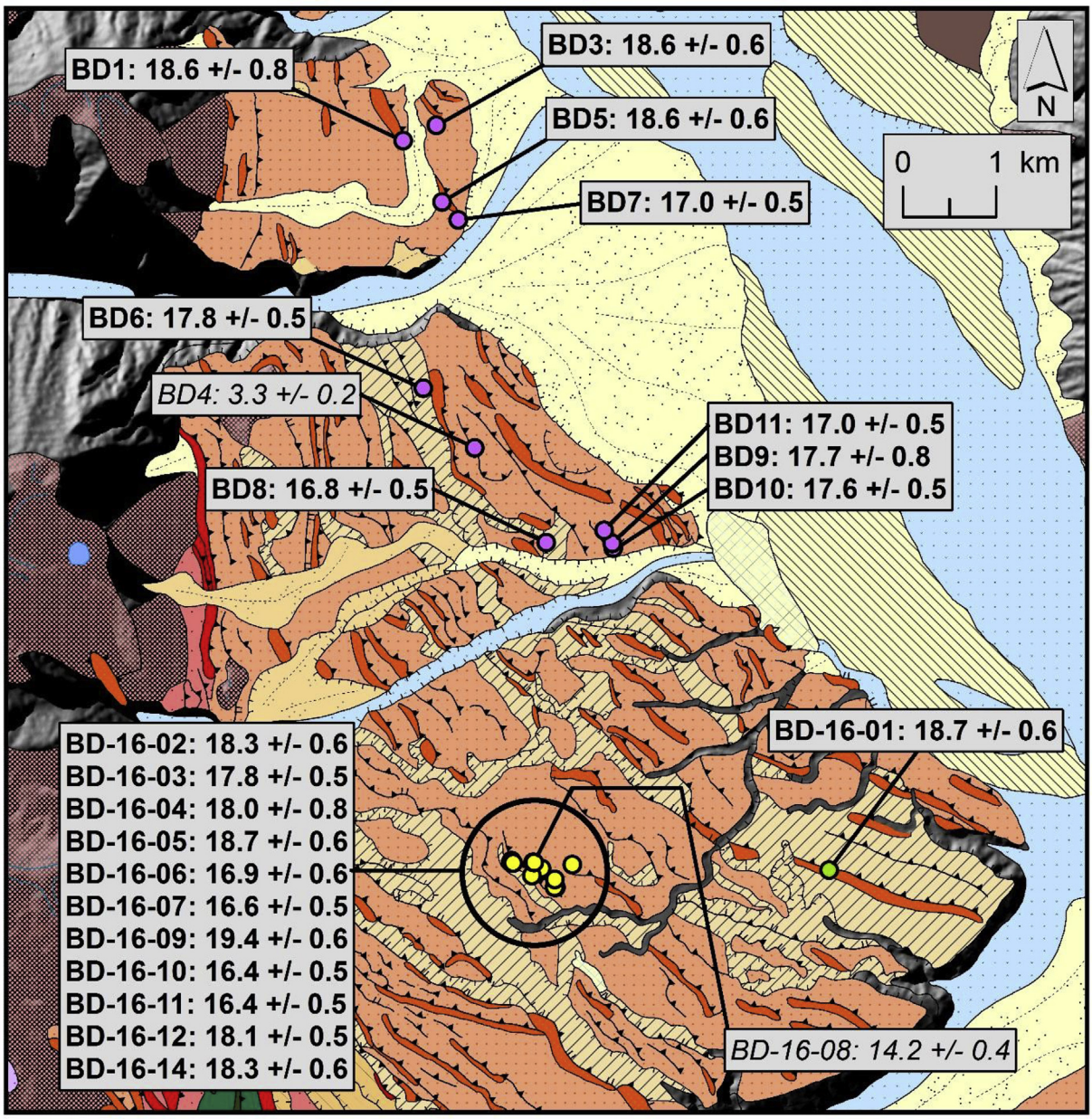

Fig. 2. Surface-exposure dating sample locations of Shulmeister et al. (2018), labelled with the sample field numbers and recalculated ages and uncertainties in kyr (this paper; Table 2), rounded to the nearest century. The two samples regarded as age outliers are labelled in plain italic font. Yellow and purple circles respectively denote samples classified here as the outer and inner groups. The one sample from a position intermediate between those groups is marked in green. Age statistics for each group are presented in Fig. 4. The base map was generated from the glacial geomorphological map dataset of Barrell et al. (2011, 2013a). Refer to Fig. 1 for location and legend. (For interpretation of the references to colour in this figure legend, the reader is referred to the Web version of this article.)

For the contour elevation estimates, we adopted the contour line elevation where the sample location coincided with a contour line, otherwise we adopted the elevation range between adjacent contours (Table 1). For the SRTM estimates, the elevation value was read off at the sample location, as viewed in Google Earth.

On 18 March 2018, we undertook field examination of all sampled boulders in the outer group at Butler Downs (Table 1). We found that the sampled boulders were at the latitude/longitude locations given by Shulmeister (2018) and the sample collection area was evident on each boulder. We measured the location and elevation of the sample collection area on each boulder using a Trimble Geo7x GPS receiver. All GPS data were differentially corrected (dGPS) against data collected at the Mount John Observatory geodetic base station, c. 48 km southwest of the outer group sampling area. Our latitudes and longitudes are reported relative to the WGS 1984 datum, and dGPS elevations are referenced to mean sea level. Horizontal and vertical uncertainties (1σ) of the measured dGPS locations are $\pm$ 0.1 m, except for sample site BD-16-14, where the vertical uncertainty is $\pm$0.8 m. Each dGPS elevation (Table 1) is that of the sampled area on each boulder.

There is good consistency between the elevations estimated from the topographic contours, the SRTM DEM and the dGPS measurements (Table 1). The SRTM estimates are routinely between 4 and 11 m lower than the dGPS values. This may reflect that SRTM elevations are relative to the ellipsoid, whereas the topographic contour elevations and dGPS elevations are referenced to a

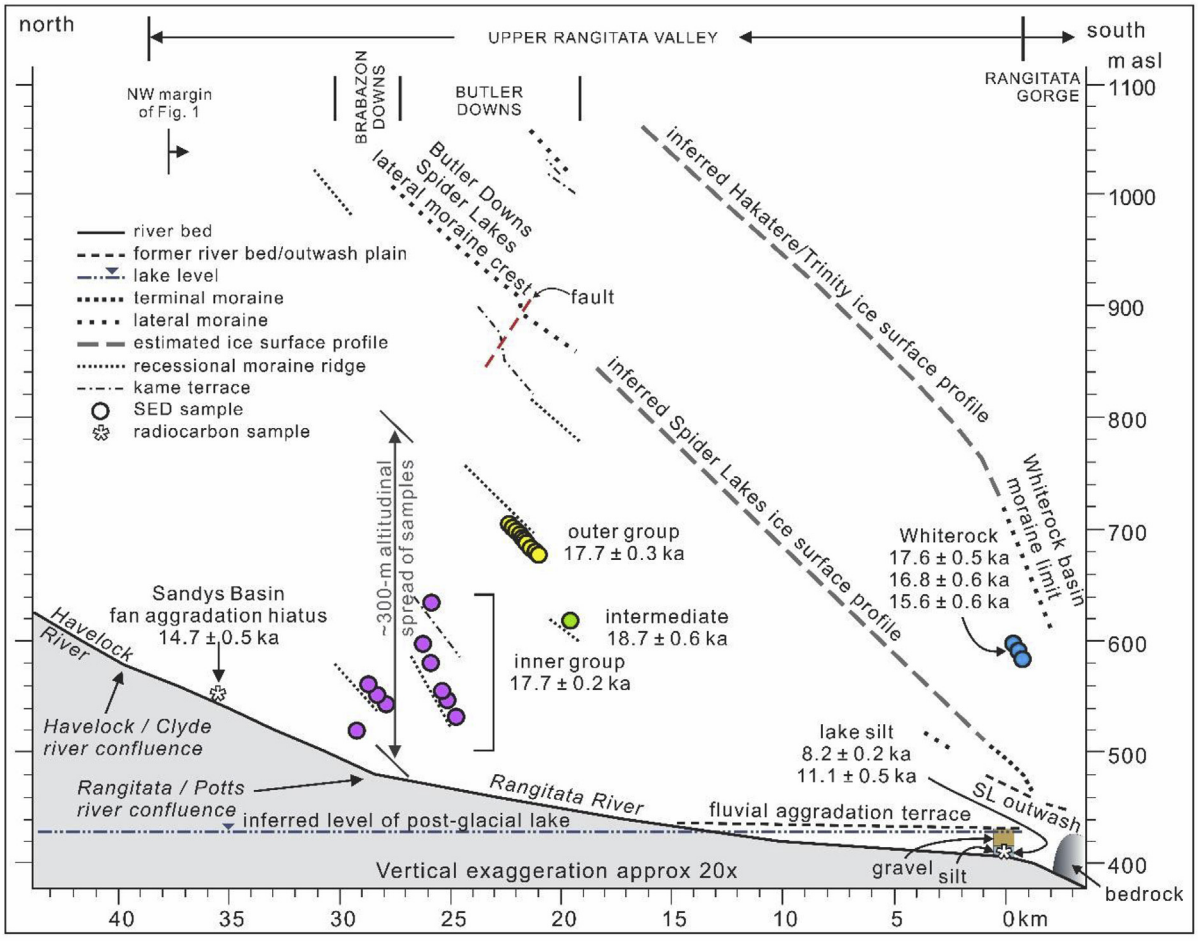

Fig. 3. Long profile of the upper Rangitata valley (location in Fig. 1). The 0 mark is at the lake sediment exposure (location C in Fig. 1). Elevations are from 20-m interval topographic contours on the Topo 50 map series. Individual moraine ridges and kame terraces are plotted where they are sufficiently continuous to intersect at least two 20-m contour intervals. Most of the ridges and terraces (Fig. 2) are too discontinuous for their gradient to be defined. The SED ages are the recalculated ('new') values from Table 2. The Whiterock ages are presented in descending elevation, comprising samples RAN-WR-3, RAN-WR-1 and RAN-WR-2 respectively (Table 2). The down-valley spread of the outer group samples is c. 1 km (Fig. 2) but is shown here slightly exaggerated to c. 2 km, to allow better illustration of the number of samples.

sea level datum. The variability in difference with dGPS values likely highlights imprecision in the SRTM model. The convergence of these three independent sources of elevation information highlights that each is reliable within their inherent uncertainties. For selecting elevations for recalculating sample ages, we used our dGPS values where available (all the outer group samples). For the other samples, we used the elevations given by Shulmeister (2018) where they are within 20 m of the topographic contour and SRTM estimates. Of the inner group and intermediate samples, only two failed to meet this test, and for those, we employed the topographic contour elevations (Table 1). The location of sample BD5 coincides with a contour line and we used that contour value. The sample BD8 location is between adjacent contour lines and we applied the mid-point of the contour elevation range. In both s, we regard the uncertainty as ± 10 m.

In our age calculations, individual ages are presented with internal errors only, relative to the year of sampling (2012 and 2016 for sample sets BD- and BD-16 respectively; Shulmeister, 2018). Calculated ages for moraine groups (Fig. 4) are presented as mean age with the standard error of the mean. Other statistics, including the mean with one standard deviation, are also shown in Fig. 4. We did not apply an erosion rate correction, in keeping with our previous work. The reasoning is that the Putnam et al. (2010) production-rate calibration did not use an erosion rate, and therefore any universal effects of erosion on Southern Alps greywacke lithologies are incorporated into the production rate. The erosion rate correction of 1 mm/kyr used in the original age calculations, as revealed in the Shulmeister (2018) data input file, adds as much as 300 years to the mean ages. This is illustrated by the difference between original versus new age in Table 2, for samples where the same elevation was used in both calculations, because we did not use an erosion rate in our recalculation. Shulmeister et al. (2018) identified only one age outlier (sample BD4), but we also identify sample BD-16-08 as an outlier, because its age is anomalously young compared to the ages obtained from all nearby samples, based on either the original calculation or the recalculations presented here (Table 2).

4. Discussion of age recalculations

On Fig. 2, the recalculated age and uncertainty for each sample is rounded to the nearest century. Comparison of the original and recalculated ages (Table 2) shows that the Shulmeister et al. (2018) ages for samples in the outer group become between 1500 and 3000 years younger after employing accurate elevations in age calculations. The recalculated mean ages and the standard errors of the means for the outer group and inner group samples (Fig. 4) are 17.7 ± 0.3 ka and 17.7 ± 0.2 ka, respectively. The spread of individual

Table 2
SED sample ages and uncertainties ('error') in years for the upper Rangitata valley. Sample ID, and calculated ages and uncertainties presented by Shulmeister et al. (2018) are identified as "original", based on elevations given in the Shulmeister (2018) data repository. Recalculated ages and uncertainties presented here are identified as 'new', based on elevations indicated in bold in Table 1. * indicates a sample whose age, shown in italics, is an outlier and is excluded from calculation of mean values. Note that the original age of sample BD-16-08 was not interpreted as an outlier. Simple arithmetic means are presented in this table and differ from the statistically calculated values in Fig. 4 which are discussed in the text. Using elevations indicated in Table 1, there is no discernible difference in mean age between the inner and outer groups. We include three ages reported by Rother et al. (2014), from the Whiterock basin (Fig. 1), recalculated on the same basis as we have done for the Shulmeister et al. (2018) ages.

Sample ID	Original age	Original age error	New age	New age error
Samples from inner group of moraines				
BD1	18900	900	18606	771
BD3	18880	730	18594	576
BD4*	*3230*	*230*	*3285*	*225*
BD5	17750	710	18615	607
BD6	18080	880	17815	534
BD7	17170	650	16960	515
BD8	17530	670	16791	509
BD9	17900	920	17659	804
BD10	17820	670	17579	526
BD11	17230	650	17016	510
MEAN	**17918**	**753**	**17737**	**595**
Sample from intermediate moraine				
BD-16-01	18990	720	18686	561
Samples from outer group of moraines				
BD-16-02	21600	860	18289	595
BD-16-03	20960	790	17773	533
BD-16-04	20130	970	17974	757
BD-16-05	20950	800	18650	572
BD-16-06	18860	780	16885	584
BD-16-07	18570	710	16622	504
BD-16-08*	15790	590	*14197*	*425*
BD-16-09	21760	840	19361	603
BD-16-10	18350	690	16422	491
BD-16-11	18350	690	16435	492
BD-16-12	20250	760	18082	541
BD-16-14	20460	810	18258	591
MEAN	**19669**	**774**	**17705**	**569**
Samples from the Whiterock basin				
RAN-WR-1	17157	785	16766	630
RAN-WR-2	15970	777	15591	639
RAN-WR-3	17913	615	17619	474

ages in each group is highlighted by the respective recalculated mean and one standard deviation values of 17.7 ± 1.0 and 17.7 ± 0.7 ka.

The context of the dating results is illustrated on a long profile of the upper Rangitata valley (Fig. 3), along with three SED ages (Table 2) from the Whiterock basin (Rother et al., 2014). Those samples were collected just inboard of, and c. 50 m lower in elevation than, a prominent lateral moraine that marks the maximum extent of presumed LGM moraines in the Whiterock basin distributary lobe of the Rangitata glacier, classified as Trinity/Hakatere moraine sets (Mabin, 1980; Barrell et al., 2011, 2013a). The Whiterock basin moraine limit is well outboard of the upper Rangitata valley Spider Lakes moraine belt (Figs. 1 and 3), suggesting that at least the two younger of those ages are unreliably young. The Spider Lakes (SL) terminal moraine at the entrance to the Rangitata Gorge is inferred to connect with the lateral moraine crest at Butler Downs, inboard of which is a landform array interpreted to reflect sustained ice recession (Fig. 5). This inferred connection accords well with the gradient of the lateral moraine crest. Taking account of ice surface gradients, there is a c. 300-m altitudinal spread of the outer and inner group samples of Shulmeister et al. (2018). The recalculated ages imply that at c. 18 ka, the surface of the Rangitata glacier lowered by at least c. 300 m, over a period within the dating uncertainty between the outer and inner groups of samples. Furthermore, the landform gradients imply that during the downwasting, the glacier must have been terminating in the developing post-glacial lake (see Section 6).

Fig. 4 compares the recalculated upper Rangitata SED ages with published ages for the onset of sustained glacier retreat in the Rakaia valley (Putnam et al., 2013a) and the Ohau valley (Putnam et al., 2013b). Overall, the recalculated upper Rangitata SED ages are compatible with glacial chronologies obtained from nearby Southern Alps valleys, and other paleoclimate proxies marking the end of the NZ LGM at c. 18 ka, as documented in detail by Barrell et al. (2013b). Accordingly, the corrected ages of the upper Rangitata SED samples imply substantial decline of the Rangitata glacier shortly after c. 18 ka, thereby challenging the main interpretations of Shulmeister et al. (2018). Further, Shulmeister et al. (2018) note that their calculated ages undermine conclusions drawn from previously reported SED ages for recession of the Clearwater distributary lobe of the Rangitata glacier (Rother et al., 2014). This is even more strongly the case with the recalculated ages presented here. The "late demise of New Zealand's last glacial maximum", a key aspect of the Rother et al. (2014) interpretation, should now be set aside, along with the main conclusions of Shulmeister et al. (2018).

5. Review of geomorphologic mapping interpretations

A discrepancy exists between the geomorphologic context of the sample sites described by Shulmeister et al. (2018) and what is shown on their maps (also see Borsellino et al., 2017). Their Fig. 3 delineates three interpretive glacial geomorphic units labelled kames (upper part of the landform sequence), kettles (also called "*dead-ice topography*"), and lateral moraines (lower part of sequence); we also note that in the caption, the descriptions of insets a) and c) are transposed. Although all dating samples are described as coming from the lower "lateral moraine" sequence, comparison between their Figs. 2 and 3 shows that what we refer to as the outer group lies within so-called "dead-ice topography". In the immediate vicinity of the outer group SED sample sites in their Fig. 2, three lines denote what are called "observed" ice limits. The presence of ice-margin landforms is at odds with an interpretation that the terrain there was produced by the ablation of a dead ice mass. A previously published geomorphologic map (Barrell et al., 2011, 2013a; our Figs. 1 and 2) records ice-contact slopes or moraine ridges at approximately the locations of the Shulmeister et al. (2018) ice limits, indicating convergence of that aspect of interpretation. Our mapping does not highlight any striking morphological difference between the intermediate and lower geomorphic units in Fig. 3 of Shulmeister et al. (2018). Overall, the presence of ice-margin landforms is difficult to reconcile with an interpretation that the terrain relates to decay of stagnant ice, rather than withdrawal of an active glacier margin.

Our geomorphological map and valley profile (Figs. 1–3) show an array of ice-marginal moraines, outwash channels and terraces within the ice recession landform sequence of the upper Rangitata valley, particularly well preserved on Butler Downs and Brabazon Downs, and classified as the 'Spider Lakes' landform set (Fig. 5). Similar landform arrays occur in the Rakaia, Pukaki and Ohau valleys, among others, inboard of the late LGM (c. 18 ka, where dated) terminal and latero-terminal moraine belt (Barrell et al., 2011, 2013a). Dating in the Rakaia and Ohau valleys (Putnam et al. (2013a, 2013b) shows that a comprehensive array of ice-margin landforms can be formed alongside a glacier that is rapidly receding, and we see no reason for interpreting the upper Rangitata valley landforms differently. Moreover, the orderly succession of those landforms, as well as those of the Pukaki valley (Barrell and Read, 2014; Doughty

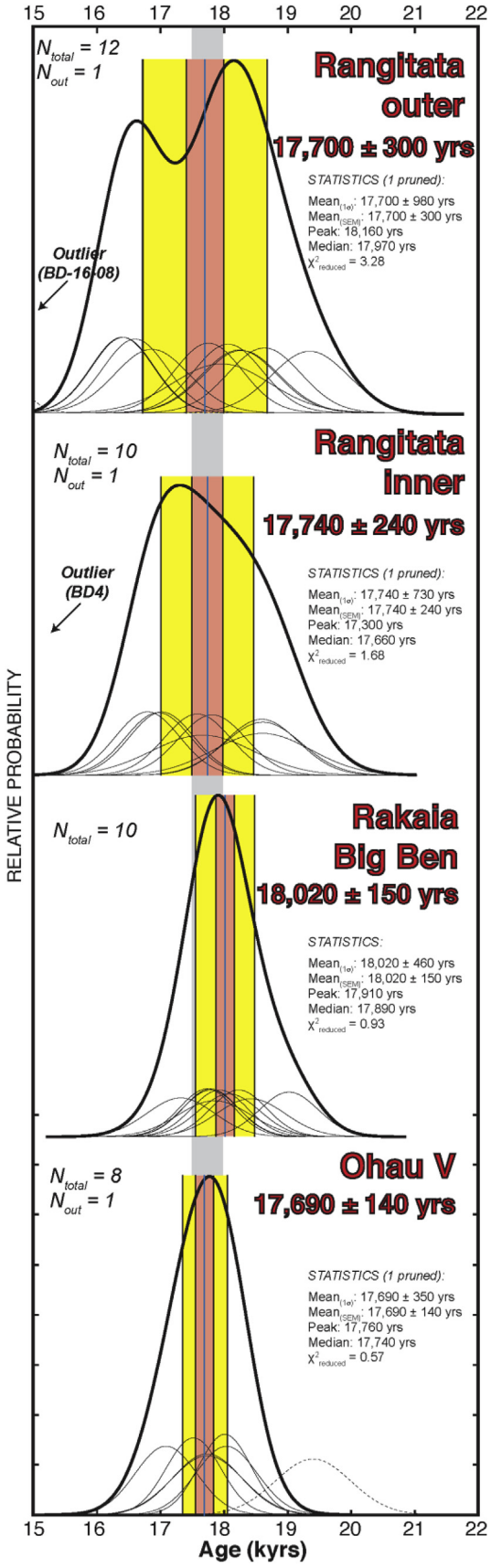

Fig. 4. Comparison of ^{10}Be surface-exposure-age distributions from late LGM moraine sets of the Rangitata (recalculated from Shulmeister et al., 2018), Rakaia (Putnam et al., 2013a), and Ohau (Putnam et al., 2013b) valleys. N refers to the number of samples analysed, and N_{out} is the number of outlier samples. Thin gaussian lines represent individual exposure ages and corresponding one-sigma analytical uncertainties. Thick black lines are summed probability curves for each 'pruned' data set (i.e., any outliers removed). Vertical yellow bands correspond to the one-sigma uncertainty limits of each summed probability curve, while the vertical orange bands are the limits of the standard error of the mean. The vertical grey band behind the main panels is the standard error of the mean for the inner Rangitata moraine group, shown to aid visual comparison with the other data sets. The large-format age labels are the mean and standard error of the mean. Note that despite the large spread in individual ages, the Rangitata age populations are normally distributed and appear indistinguishable from age populations of geomorphologically similar moraine belts of the Rakaia and Ohau valleys. (For interpretation of the references to colour in this figure legend, the reader is referred to the Web version of this article.)

et al., 2015), is more suggestive of progressive recession of an active glacier margin, rather than a catastrophic calving-related retreat.

We regard the 'Spider Lakes' landform set of the Rangitata glacial system, as delineated in the Barrell et al. (2011, 2013a) geomorphological map (Figs. 1 and 2), as likely representing the last substantial advance of the Rangitata Glacier, followed by sustained retreat (Figs. 3 and 5). All the samples analysed by Shulmeister et al. (2018) lie within what we interpret, morphologically, as the deglacial landform set of the Rangitata Glacier system.

6. Deglacial and post-glacial landscape of the upper Rangitata valley

6.1. The question of a post-glacial lake

In interpreting the SED ages for the Rangitata glacier system, Rother et al. (2014) and Shulmeister et al. (2018) contend that the upper Rangitata valley did not contain a large post-glacial lake. They thereby viewed the Rangitata moraine chronologies as being more reliable indicators of Southern Alps paleoclimate than moraine chronologies from valleys with post-glacial lakes. As part of the reasoning that a large post-glacial lake did not form in the upper Rangitata valley, Shulmeister et al. (2018; their Section 4.2) state: "*bedrock crops out in the floor of the main Rangitata Valley only a few kilometres upstream of the Brabazon Downs and it is expected that the fluvial valley fill along the line of the main channel of the Rangitata is thin in this valley reach*". However, Fig. 1 highlights that there are only small areas of bedrock outcrop in the upper Rangitata valley floor, relative to the overall width of the valley. The published geological map (Cox and Barrell, 2007; Heron, 2014) shows that aside from a few knobs of bedrock protruding from the valley floor, Holocene river sediments, flanked by Holocene alluvial fans or landslide debris, occupy the main valley floor of the Rangitata, and its main feeder tributaries of the Havelock and Clyde rivers, well into the headwaters. The geological mapping evidence provides no foundation for inferring that the upper Rangitata valley has a shallow depth of post-glacial sediment fill.

The inference that there was no post-glacial lake is summed up in Section 4.3 of Shulmeister et al. (2018): "*the Rangitata Valley does not contain a trough which could constrain a persistent glacial lake, at least upstream of the Rangitata Gorge. Thus, when the glacier retreated into the bedrock-confined upper Rangitata Valley, its ice volume thinned and retreated continuously.*" However, this view conflicts with the findings of Mabin (1987), who described the stratigraphy and radiocarbon dating of post-glacial lake sediments exposed at the downstream end of the upper Rangitata valley (Figs. 3 and 6). Mabin documented a stratigraphic section comprising 14.5 m of horizontally bedded, slightly iron-stained, rounded greywacke gravels, resting on at least 12 m of irregularly bedded, laminated grey clays. The lower unit, interpreted as a lacustrine deposit, contains plant and wood

Fig. 5. View looking northwest across the glacial landforms of Butler Downs. Sample BD-16-05 was collected from this boulder, and the white GPS antenna sits on the sample collection site. The arrows mark the crest of a prominent lateral moraine wall which is mapped as the upper limit of the Spider Lakes landform set. We interpret the landforms below that moraine wall crest as having become exposed following the onset of sustained ice recession associated with deglaciation in this valley. The ellipse highlights a flight of alluvial fan terraces interpreted as having graded to a progressively lowering ice margin. This boulder sits about 200 m below the level of the morphological break (see Fig. 3). Photo GNS Science, D.J.A. Barrell, March 2018.

fragments, and the overlying gravels and sands were interpreted as a fluvial aggradation deposit. Mabin (1987) reported radiocarbon ages from the lacustrine sediments at heights above river level of 3.5 m (9780 ± 140 years B.P.; NZ5406A) and 11.25 m (7380 ± 110 years B.P.; NZ5405A). These equate respectively to SHCal13 (Hogg et al., 2013), 95% probability, age ranges of 10 678– 11 608 cal. yr B.P. and 7965–8370 cal. yr B.P. Rounding the interval between the two calibrated age ranges to 3 kyr implies an average sedimentation rate of 1 m per c. 390 years (i.e. 2.6 mm/yr). The Rangitata River has a contemporary suspended sediment yield of 1.576 million tonnes (t) per year (Hicks et al., 2011). As a hypothetical estimate, assuming a nominal density of deposited sediment of 2 t/m^3, if 1.576 Mt of suspended sediment was deposited evenly across the bed of a standing water body at 2.6 mm/yr, it would require a bed surface area of c. 30 km^2. Although a very simplistic hypothetical estimate, it provides a basis for inferring that the post-glacial lake which occupied the upper Rangitata valley was large.

Close to the gorge entrance, Mabin (1987) reported that the lake sediment rests on poorly sorted gravel that he interpreted as glacial

Fig. 6. Riverbank exposure of light grey lacustrine sediment, with some sandy interbeds, overlain by light grey to yellow brown fluvial sand and gravel, at latitude and longitude 43.735°S, 171.182°E (locality C in Fig. 1), at the approximate location of the site described by Mabin (1987). This c. 20 m high exposure occurs beneath a c. 30 m high river terrace (background) and is partly draped by an active dune of river sand. The active bed of the Rangitata River is in the foreground. Photo GNS Science, D.J.A. Barrell, May 2002. (For interpretation of the references to colour in this figure legend, the reader is referred to the Web version of this article.)

till. Mabin's (1987) overall interpretation, which refers to the Otira Glaciation climate stage of New Zealand (approximately spanning MIS 4 to MIS 2) and is based on uncalibrated radiocarbon age determinations, was that: "*the Rangitata glacier receded from its late Otiran advance position well before 11 450 years ago. As it receded, a lake became impounded behind the moraines that blocked the head of the gorge and extended for at least* 14 km *upvalley to the area of Forest Creek*" (see Fig. 1).

The downstream three-quarters of the Rangitata Gorge (Fig. 1) is floored by greywacke bedrock (Oliver and Keene, 1990; Cox and Barrell, 2007; Heron, 2014), and post-glacial incised strath terraces cut on greywacke bedrock (represented schematically in Fig. 3) stand as much as 40 m above modern river level (Barrell et al., 1996). No bedrock is exposed in the upstream one-quarter of the gorge floor, with river cliffs formed in Quaternary deposits. The geomorphology comprises extensive remnants of moraine and outwash terraces correlated with the Spider Lakes landform group (Mabin, 1980, 1987). These observations led Barrell et al. (1996) to interpret those moraines as sitting near the downstream margin of a glacially-excavated trough that underlies the upper Rangitata valley. Collectively, the prominent bedrock floor and strath terraces of the mid to downstream sector of the gorge, when compared to the extensive absence of bedrock outcrop in the upper valley, point strongly towards the presence there of a glacial trough.

In the Rangitata Gorge, a large landslide deposit sits on the Spider Lakes outwash terrace. Although Barrell et al. (1996) left open the question of whether the lake in the upper Rangitata valley was impounded behind glacial deposits, or by the landslide, subsequent fieldwork at the downstream end of the gorge (Barrell, unpublished) revealed a fluvial aggradation deposit composed of angular gravel, interpreted as reworked landslide debris, at about the same level as the terrace upon which the landslide rests. This deposit indicates that fluvial breach and downstream redistribution of the landslide debris occurred before the river system became notably incised into the Spider Lakes glacial outwash train. Thus, we consider that impoundment behind moraine, and the in-situ bedrock of the gorge downstream of the glacial trough, is the most likely context for the post-glacial Rangitata lake.

6.2. Post-glacial evolution of the upper Rangitata landscape

The field evidence and conclusions of Mabin (1987) and Barrell et al. (1996) invalidate the interpretation of Rother et al. (2014) and Shulmeister et al. (2018) that the upper Rangitata valley did not hold a post-glacial lake and that the Rangitata glacier system was therefore different to glacier systems of other nearby valleys. The collective geological and geomorphological evidence points towards a substantial glacially-excavated trough in the upper Rangitata valley, extending well up-valley. Rapid ice recession, indicated as having been in progress at c. 18 ka by the recalculated SED ages at Butler Downs and Brabazon Downs, likely heralded the initiation of the post-glacial lake. The evidence of Mabin (1987) that the lake persisted at least into the early Holocene implies that the lake was sufficiently large to have accommodated the substantial sediment yield of the Rangitata catchment for at least c. 10 kyr. The presence of fluvial sediments above the lake sediment exposure (Fig. 6) suggests that the lacustrine episode was terminated by infilling of the lake as the Rangitata River prograded down and through to the lake outlet (fluvial aggradation terrace in Fig. 3). That terrace, and incised degradation surfaces below that level, extend up-valley but at noticeably lesser gradient than the modern river bed, and intersect the valley floor just downstream of the Forest Creek confluence (Fig. 1). By this reasoning, the elevation of the fluvial terrace at the lake sediment exposure, which we estimate as c. 430 m asl) from topographic map contours, and within a kilometre upstream of the former lake outlet, should be a close approximation of the former lake level. The genetic model we envisage is that the level of the post-glacial lake was initially maintained by bedrock in the gorge floor (Fig. 3), with incision into bedrock greatly inhibited by the absence of sand and gravel bedload, which was being trapped in the lake. Progradation of the river delta through the lake delivered coarse bedload to the gorge, facilitating incision, that eventually retrograded some 14 km or so upstream of the gorge entrance, to where the terraces merge with the modern riverbed. We consider that the minimal geomorphic signature of the lake in the upper Rangitata valley is because the lake sediments and landforms have largely been buried by fluvial sedimentation (Fig. 3).

The only other documented insight into landscape conditions in the upper Rangitata valley during the last glacial – interglacial transition (c. 18 – c. 11.9 ka; Barrell et al., 2013b) comes from an exposure of alluvial fan deposits derived from Sandys Basin, a small valley-margin catchment of about 1.5 km^2, c. 6 km up-valley from Brabazon Downs (Figs. 1 and 3). There, radiocarbon dating of a well-developed soil buried within the fan deposits (Forsyth et al., 2003), on samples of wood (Wk 10872; 12 552 ± 133 yr BP) and leaf fragments (NZA 15192; 12 624 ± 75 yr BP), yields respective SHCal13 age ranges (95% probability) of 14 159–15 180 and 14 415–15 207 cal. yr BP. These afford minima for the withdrawal of the glacier from that area, and the completion of at least one episode of alluvial fan construction out into the upper Rangitata valley. The elevation of the buried soil exposure is c. 540 m asl, estimated from topographic map contours. Mabin's (1987) evidence for a large post-glacial lake persisting in the valley until at least the Early Holocene implies that the Sandys Basin fan would likely have prograded out into the lake. As the exposed buried soil is about 100 m above indicated lake level, and the fan surface has a fall of 100 m per c. 0.5 km, we infer that at c. 14.5–15 ka, the paleo-lake shore was c. 0.5 km valley-ward of that location but is now buried under c. 100 m of fluvial sediment. Fluvial aggradation provides an explanation as to minimal surface evidence remains for the Rangitata lake and underscores the importance of the Mabin (1987) exposure as providing one of the few recognisable traces of that lake.

7. Discussion

The application of corrected elevations and recalculation of the chronology of Shulmeister et al. (2018) indicates a substantial lowering of Rangitata glacier ice at c. 18 ka. The recalculated Rangitata chronology is thus compatible with dating results from other eastern valleys of the Southern Alps, indicating the onset of sustained ice retreat from LGM moraines at c. 18 ka that is readily attributable to climate amelioration. We also note evidence for the existence of a long-lived post-glacial lake in the upper Rangitata valley (Mabin, 1987; Barrell et al., 1996). This indicates that post-glacial lacustrine conditions existed in the upper Rangitata similarly to other nearby glacial valleys. It is, however, far from clear that post-glacial lakes have confounded moraine records of deglaciation and indeed the Southern Alps glacial landform record generally indicates otherwise. Within the Southern Alps glacial valleys, including the upper Rangitata valley, the deglacial landform sequence contains many ice-contact kame terraces, in places flanked by lateral moraines, for example in the Rakaia, Pukaki and Ohau valleys (Putnam et al., 2013a, 2013b; Barrell and Read, 2014; Kelley et al., 2014; Doughty et al., 2015). We consider it unlikely that such features would have formed beside a glacier tongue undergoing catastrophic, calving-related, collapse, but rather see them as indicative of formation alongside an active glacier margin. Overall, we conclude that the available evidence highlights that

deglaciation of the upper Rangitata valley was similar in style and chronology to that of other nearby valleys.

Acknowledgements

DB acknowledges support from the New Zealand Government through the GNS Science 'Global Change through Time' programme. We are grateful to the managers of Forest Peak Station for allowing access to Butler Downs for the inspection of sample sites. An early draft of the manuscript benefitted from comments from Simon Cox. We are grateful for comments from two anonymous referees and handling editor Neil Glasser that resulted in many improvements to the manuscript.

References

Balco, G., Stone, J.O., Lifton, N.A., Dunai, T.J., 2008. A complete and easily accessible means of calculating surface exposure ages or erosion rates from ^{10}Be and ^{26}Al measurements. Quat. Geochronol. 3, 174–195.

Barrell, D.J.A., 2011. Quaternary glaciers of New Zealand. In: Ehlers, J., Gibbard, P.L., Hughes, P.D. (Eds.), Quaternary Glaciations: Extent and Chronology - a Closer Look. Developments in Quaternary Science 15. Elsevier, Amsterdam, pp. 1047–1064.

Barrell, D.J.A., Read, S.A.L., 2014. The deglaciation of lake Pukaki, South Island, New Zealand - a review. N. Z. J. Geol. Geophys. 57, 86–101.

Barrell, D.J.A., Forsyth, P.J., McSaveney, M.J., 1996. Quaternary geology of the Rangitata fan, Canterbury Plains, New Zealand. Institute of Geological & Nuclear Sciences, Lower Hutt. Institute of Geological & Nuclear Sciences Science Report 96/23, 67 p.

Barrell, D.J.A., Andersen, B.G., Denton, G.H., 2011. Glacial geomorphology of the central South Island, New Zealand. Lower Hutt: GNS Science. GNS Science, Lower Hutt. GNS Science Monograph 27, 81 p. + map (5 sheets).

Barrell, D.J.A., Andersen, B.G., Denton, G.H., Smith Lyttle, B., 2013a. Glacial geomorphology of the central South Island, New Zealand - digital data. Lower Hutt: GNS Science. GNS Science Monograph 27a. Geographic Information System digital data files + explanatory notes. GNS Science, Lower Hutt, p. 17. GNS Science Monograph 27a, 1 CD containing Geographic Information System digital data files + explanatory notes (17 p.), Web viewer available at: www.gns.cri.nz, (search term "central South Island glacial geomorphology").

Barrell, D.J.A., Almond, P.C., Vandergoes, M.J., Lowe, D.J., Newnham, R.M., NZ-INTIMATE members, 2013b. A composite pollen-based stratotype for inter-regional evaluation of climatic events in New Zealand over the past 30,000 years (NZ-INTIMATE project). Quat. Sci. Rev. 74, 4–20.

Borsellino, R., Shulmeister, J., Winkler, S., 2017. Glacial geomorphology of the Brabazon & Butler Downs, Rangitata valley, South Island, New Zealand. J. Maps 13, 502–510.

Clark, P.U., Dyke, A.S., Shakun, J.D., Carlson, A.E., Clark, J., Wohlfarth, B., Mitrovica, J.X., Hostetler, S.W., McCabe, A.M., 2009. The last glacial maximum. Science 325, 710–714.

Cox, S.C., Barrell, D.J.A., 2007. Geology of the Aoraki area. GNS Science, Lower Hutt. Institute of Geological & Nuclear Sciences 1:250,000 Geological Map 15, 71 p. + 1 folded map.

Darvill, C.M., Bentley, M.J., Stokes, C.R., Shulmeister, J., 2016. The timing and cause of glacial advances in the southern mid-latitudes during the last glacial cycle based on a synthesis of exposure ages from Patagonia and New Zealand. Quat. Sci. Rev. 149, 200–214.

Doughty, A.M., Schaefer, J.M., Putnam, A.E., Denton, G.H., Kaplan, M.R., Barrell, D.J.A., Andersen, B.G., Kelley, S.E., Finkel, R.C., Schwartz, R., 2015. Mismatch of glacier extent and summer insolation in Southern Hemisphere mid-latitudes. Geology 43, 407–410.

Dunai, T.J., Stuart, F.M., 2009. Reporting of cosmogenic nuclide data for exposure age and erosion rate determinations. Quat. Geochronol. 4, 437–440.

Forsyth, P.J., Barrell, D.J.A., Basher, L.R., Berryman, K.R., 2003. Holocene landscape evolution of the Havelock and upper Rangitata valleys, South Canterbury, New Zealand. Institute of Geological & Nuclear Sciences, Lower Hutt. Institute of Geological & Nuclear Sciences Science Report 2003/22, 45 p.

Hall, B.L., Porter, C.T., Denton, G.H., Lowell, T.V., Bromley, G.R.M., 2013. Extensive recession of Cordillera Darwin glaciers in southernmost South America during Heinrich stadial 1. Quat. Sci. Rev. 62, 49–55.

Hall, B.L., Denton, G.H., Lowell, T.V., Bromley, G.R.M., Putnam, A.E., 2017. Retreat of the Cordillera Darwin icefield during termination I. Cuadernos de Investigación Geográfica 43 (2), 751–766.

Heron, D.W., 2014. Geological map of New Zealand 1:250,000. : . GNS Science geological map 1. 1 CD. GNS Science, Lower Hutt. GNS Science geological map 1. 1 CD, 2014, Web viewer available at www.gns.cri.nz, (search term "geology web map").

Hicks, D.M., Shankar, U., McKerchar, A.I., Basher, L., Jessen, M., Lynn, I., Page, M., 2011. Suspended sediment yields from New Zealand rivers. Journal of Hydrology (New Zealand) 50, 81–142.

Hogg, A.G., Quan, H., Blackwell, P., Niu, M., Buck, C., Guilderson, T.P., Heaton, T.J., Palmer, J.G., Reimer, P.J., Reimer, R.W., Turney, C.S.M., Zimmerman, S.R.H., 2013. SHCal13 Southern Hemisphere calibration, 0–50,000 years cal BP. Radiocarbon 55, 1889–1903.

Kelley, S.E., Kaplan, M.R., Schaefer, J.M., Andersen, B.G., Barrell, D.J.A., Putnam, A.E., Denton, G.H., Schwartz, R., Finkel, R.C., Doughty, A.M., 2014. High-precision ^{10}Be chronology of moraines in the Southern Alps indicates synchronous cooling in Antarctica and New Zealand 42,000 years ago. Earth Planet Sci. Lett. 405, 194–206.

Lifton, N., Sato, T., Dunai, T.J., 2014. Scaling in situ cosmogenic nuclide production rates using analytical approximations to atmospheric cosmic-ray fluxes. Earth Planet Sci. Lett. 386, 149–160.

Mabin, M.C.G., 1980. The glacial sequences in the Rangitata and Ashburton valleys, South Island, New Zealand. PhD thesis. University of Canterbury, 238 p.

Mabin, M.C.G., 1987. Early Aranuian sedimentation in the Rangitata valley, mid Canterbury. N. Z. J. Geol. Geophys. 30, 87–90.

Moreno, P.I., Denton, G.H., Moreno, H., Lowell, T.V., Putnam, A.E., Kaplan, M.R., 2015. Radiocarbon chronology of the last glacial maximum and its termination in northwestern Patagonia. Quat. Sci. Rev. 122, 233–249.

Oliver, P.J., Keene, H.W., 1990. Sheet J36 BD and part sheet J35, Clearwater. New Zealand Geological Survey, Lower Hutt. Geological map of New Zealand 1: 50,000, sheets J36 & part J35. Map + booklet.

Putnam, A.E., Schaefer, J.M., Barrell, D.J.A., Vandergoes, M.J., Denton, G.H., Kaplan, M.R., Finkel, R.C., Schwartz, R., Goehring, B.M., Kelley, S.E., 2010. In situ cosmogenic ^{10}Be production-rate calibration from the Southern Alps, New Zealand. Quat. Geochronol. 5, 392–409.

Putnam, A.E., Schaefer, J.M., Denton, G.H., Barrell, D.J.A., Andersen, B.G., Koffman, T.N.B., Rowan, A.V., Finkel, R.C., Rood, D.H., Schwartz, R., Vandergoes, M.J., Plummer, M.A., Brocklehurst, S.H., Kelley, S.E., Ladig, K.L., 2013a. Warming and glacier recession in the Rakaia valley, Southern Alps of New Zealand, during Heinrich stadial 1. Earth Planet Sci. Lett. 382, 98–110.

Putnam, A.E., Schaefer, J.M., Denton, G.H., Barrell, D.J.A., Birkel, S.D., Andersen, B.G., Kaplan, M.R., Finkel, R.C., Schwartz, R., Doughty, A.M., 2013b. The last glacial maximum at 44°S documented by a ^{10}Be moraine chronology at Lake Ohau, Southern Alps of New Zealand. Quat. Sci. Rev. 62, 114–141.

Rother, H., Fink, D., Shulmeister, J., Mifsud, C., Evans, M., Pugh, J., 2014. The early rise and late demise of New Zealand's last glacial maximum. Proc. Natl. Acad. Sci. U. S. A. 111, 11630–11635.

Shulmeister, J., 2018. Data for Quaternary Science Reviews Paper JQSR 5235 - evidence for slow late-glacial ice retreat in the upper Rangitata Valley, South Island, New Zealand. Mendeley Data, v1. File: shulmeister rangitata input cronus archive 15dec17.tx. https://doi.org/10.17632/t74n5p4b9y.1.

Shulmeister, J., Fink, D., Winkler, S., Thackray, G.D., Borsellino, R., Hemmingsen, M., Rittenour, T.M., 2018. Evidence for slow late-glacial ice retreat in the upper Rangitata Valley, South Island, New Zealand. Quat. Sci. Rev. 185, 102–112.